Application of digital signal processing in discrimination of neutrons and gamma rays

Amiri, M. & Přenosil, V.

Original citation & hyperlink:
Amiri, M & Přenosil, V 2015, Application of digital signal processing in discrimination of neutrons and gamma rays. in 38th International Conference on Telecommunications and Signal Processing (TSP). IEEE, 38th International Conference on Telecommunications and Signal Processing, Prague, Czech Republic, 9/07/15.
https://dx.doi.org/10.1109/TSP.2015.7296441

DOI 10.1109/TSP.2015.7296441
ISBN 978-1-4799-8498-5

Publisher: IEEE

Application of Digital Signal Processing in Discrimination of Neutrons and Gamma Rays

Moslem Amiri, Václav Přenosil

***Abstract*—Two new methods for the digital discrimination of neutrons and gamma-rays in a mixed radiation field using digital signal processing techniques are presented. While almost all of the pulse-shape discrimination methods use time-domain features of signals, the proposed procedures successfully separate these radiations using their frequency-domain data. These methods are computationally simple, hence appropriate for field measurements. Applied to several sets of mixed neutron and photon signals obtained through different digitizers using stilbene scintillator, these approaches are analyzed and their discrimination qualities are measured.**

***Keywords*—Digital signal processing, Discrimination technique, Frequency domain data, Neutron spectroscopy, Organic scintillator.**

I. Introduction

THE range of applications of neutron detectors grows fast. Nowadays, neutron detectors are used for neutron imaging techniques, nuclear research, nuclear medicine applications, and safety issues, and their usage spans on various branches of science including nuclear physics, biology, geology, and medicine. The main problem in neutron detection is the discrimination of neutrons from the background gamma rays. Fast neutrons produce recoil protons whose detection is the most common method to detect neutrons. Organic scintillators are widely used to detect these recoil protons. Fast neutrons in organic scintillators produce recoil protons through (n, p) elastic scattering and energy of a recoil proton at the highest level is equal to the energy of the neutron [1].

Among organic scintillators, stilbene and NE-213 come with some advantages for neutron spectroscopy purposes; they have rather low light output per unit energy, but this light output induced by charged protons can be easily distinguished from electrons/photons. Hence, stilbene and NE-213 scintillators produce very good results using pulse shape discrimination (PSD) methods.

Time-domain PSD methods are not computationally intensive, and hence are suitable for real-time applications. Classically, following analog PSD techniques were most often used for n/γ-ray discrimination [2]:

1) rise-time inspection;
2) zero-crossing method;
3) charge comparison.

Although analog techniques make acceptable n/γ-ray discrimination, availability of precise and fast digitizers and various PSD algorithms have made it possible to do a better discrimination of these radiations digitally. Among digital PSD methods, pulse rise-time algorithm and charge comparison are probably the most favorable ones.

In this paper, we introduce two computationally-simple frequency-domain-based discrimination methods, and calculate their separation qualities. To obtain the sampled data of mixed neutron and gamma-ray pulses, we use two differently-featured digitizers: Acqiris DP210 with 8-bit resolution and set at 1 and 2 GSamp/s, and Acqiris DC440 with 12-bit resolution and set at 250 and 420 MSamp/s. Doing so, we could find the effect of resolution and sampling frequency of the digitizers on the quality of the discrimination results for our novel methods. Every experiment is carried out using 100,000 pulses of mixed neutron and photon signals. Stilbene scintillation detector was used with 45x45 crystal, and the neutron-gamma radiation source used was 252Cf.

A comparison among various techniques, applied to data obtained from the different digitizer types and settings, is done by using the Figure of Merit (FoM) for the neutron/gamma discrimination, defined as:

$$FoM = \frac{S}{FWHM_n + FWHM_\gamma} \tag{1}$$

where S is the separation between the peaks of the two events, $FWHM_\gamma$ is the full-width half-maximum (FWHM) of the spread of events classified as gamma-rays and $FWHM_n$ is the FWHM of the spread in the neutron peak [3]. FWHMs are calculated using the Gaussian fits to the neutron and gamma-ray events on experimental distribution plot.

II. Neutron and Photon Signals

A sample smoothed neutron is compared with a sample smoothed photon pulse in Fig. 1. These signals are obtained from the stilbene scintillator. As seen in this Figure, these signals are composed of a rising and a trailing edge. The rising edges could not be exploited for discrimination purposes. However, the trailing edge of the neutron signal has higher rise time than that of the photon signal. This property could be used to separate these two radiations. However, this difference is not large enough to be exploited by directly applying signal processing techniques.

An innovative approach for discrimination is to remove the similar segments of the two signal types and apply the technique only to the differing segments. Fig. 2 shows a short segment of a normalized unknown pulse which could be used for discrimination. The two ends of this segment are constant amounts of time after the signal reaches a specified level on the rising edge.

Manuscript received April 21, 2014. This work was supported by Technology Agency of the Czech Republic under contract No. TA01011383/2011.

M. Amiri and V. Přenosil are with the Faculty of Informatics, Masaryk University, Brno, Czech Republic (e-mail: amiri@mail.muni.cz; prenosil@fi.muni.cz).

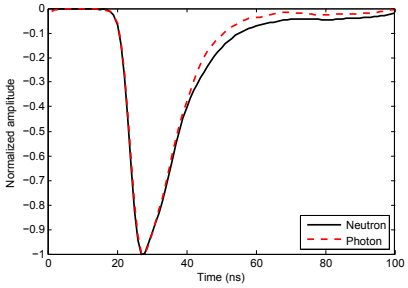

Fig. 1. Comparison of a sample smoothed neutron with a sample smoothed photon. These signals are obtained from the stilbene scintillator.

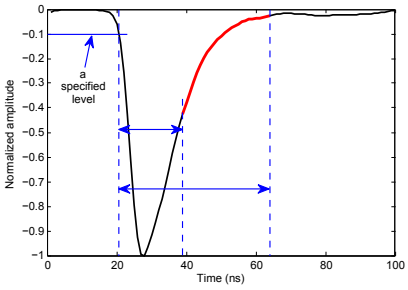

Fig. 2. Segment of an unknown signal, shown in bold red, to be used in our discrimination method.

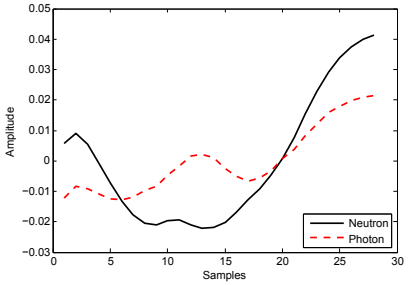

Fig. 3. Neutron and photon signal segments, obtained under 12-bit resolution and 420 MS/s sampling rate, after mean of the windowed curve is subtracted from every point.

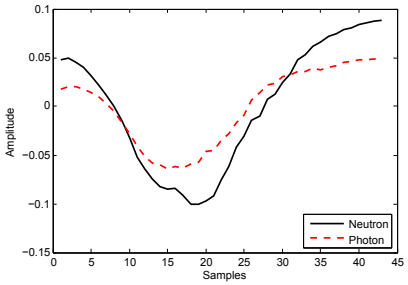

Fig. 4. Neutron and photon signal segments, obtained under 8-bit resolution and 1 GS/s sampling rate, after mean of the windowed curve is subtracted from every point.

III. Application of FFT Method

In this Section, we introduce a discrimination method based on the frequency-domain data. We apply FFT (fast Fourier transform) only to a short segment of the normalized pulses (Fig. 2); as explained in Section II, the two ends of this segment are determined by adding two constant amounts of time to the point when a specified level on the rising edge is reached. Determination of a specified level on the rising edge as the starting point is arbitrary because the two rising edges of neutrons and photons are almost the same. Some training pulses are used to find the two constant amounts of time after the starting point within which the differing segments of neutrons and photons exist. In our experiments, this segment falls on the trailing edge from about 2% to 40% of peak-amplitude, on average. However, changing these boundaries will not have a significant effect on the result. Given this segment, the following steps are taken:

1) Hamming window is applied to the said segment of the normalized pulse;
2) Mean of the windowed curve is subtracted from every point;
3) The signal is padded with enough number of zeros to make the total number of points a power of two;
4) FFT is taken.

In Step 1, the Hamming window is used because it is raised on a pedestal. This property of Hamming window helps retain the sloped shape of the cuts of the two radiation types (red segment in Fig. 2) as much as possible. As we will explain, this sloped shape helps exploit the differences between the radiation types.

In Step 2, the mean of curve is subtracted from every point *after* application of window, while typically this is performed *before* window application (for removal of DC spectral component). This will cause the left ends of the neutron and photon pulses get opposing amplitude signs, as Fig. 3 illustrates. Since the samples with lower indexes have higher frequencies, the different signs of neutrons and photons will create a mirror image of them in high frequency region of their spectra. Although this difference could be easily used for discrimination, mid-samples in Fig. 3, which contribute to the lower frequencies, have this property too. This difference is not always achievable: it depends on the resolution of the data, the length of the segment used, and the instrumentation settings. Fig. 4 shows the result of the same approach applied to the data obtained with 8-bit resolution digitizer set at 1 GSamp/s sampling rate. Digital signal processing techniques almost fail to discriminate in such cases. In Section IV, we will introduce a general approach to resolve this issue.

Fig. 5 shows the magnitude spectra of two sample neutron and photon pulses obtained by DC440 digitizer (set at 420 MSamp/s). As seen in this Figure, the peaks of the lobes of the γ-ray pulses have lower frequencies than neutrons (specially in low-frequency region). This fact could be easily used to distinguish the two signals. However, as pointed out earlier, the interesting event occurs in the higher frequencies, especially in the final lobe; the two lobes are mirror images of each other. The spectra of Fig. 5 is the result of a 64-point FFT; if we apply higher number of FFT points (by padding more zeros), this mirror image event is still happening, only that it is more detailed, and every lobe is comprised of more number of points. An easily measurable discrimination factor would be the slope of the line connecting the peak and the valley of the last lobe at the highest frequency. In the case of Fig. 5, the

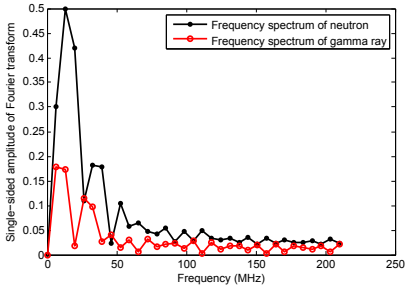

Fig. 5. The magnitude spectra of γ-ray events and neutron events, applying a 64-point FFT. The pulses are obtained using DC440 digitizer (12-bit resolution, 420 MSamp/s).

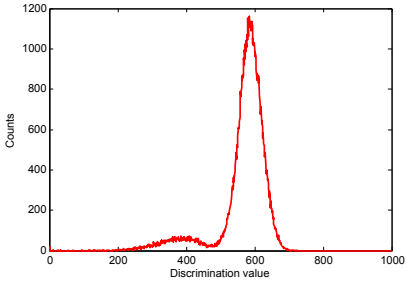

Fig. 6. Discrimination of photon and neutron signals, applying a 64-point FFT. The pulses are obtained using DC440 digitizer (12-bit resolution, 420 MSamp/s). For this work, the field consists of mostly gamma rays and some neutrons. This higher ratio of gamma rays to neutrons is reflected in this experimental distribution plot.

discrimination factor is simply the subtraction of amplitude of $(N/2)$th point from the amplitude of $(N/2-1)$th point in an N-point FFT. The advantages of this approach are:

1) It is simple. Even with low number of points in FFT, this method works;
2) The amplitude of only two bins is enough for the discrimination. Therefore, there is no need for full-spectrum FFT calculation. Employing methods like Goertzel algorithm is enough to do the required measurements while keeping the process simple.

In Tab. I, the FoMs for 12-bit resolution data are obtained using the method explained above, i.e., the slope of the line connecting the bins $N/2-1$ and $N/2$. A 64-point FFT is used for the data obtained using the DC440 digitizer with 12-bit resolution and at 420 MSamp/s, and a 32-bit FFT is used for the data obtained using the same digitizer but at 250 MSamp/s. Fig. 6 shows the discrimination plot for the data obtained at 420 MSamp/s. As explained before, while this mirror image of the spectra in the higher frequency region is an easy approach to distinguishing neutrons and photons, this property cannot be used for the data obtained using digitizers featuring lower-resolution, e.g., 8 bits. For low-resolution data, the mirror image does not occur consistently with neutrons and photons. In high-resolution data, even the differences in low-frequency region can be easily used to discriminate the pulses, as Fig. 5 illustrates, but in low-resolution data, this difference is not enough for proper discrimination.

Another discriminating factor which could be exploited for any type of data, either the ones with low- or high-resolution, is the magnitude difference between the neutron and photon pulses; since the cut shown in Fig. 2 has higher average magnitude for neutrons than photons, this difference is also reflected in frequency domain (in zero frequency, i.e., the mean of the samples). In order to exploit this reflection, the second step in our method explained above, i.e., the subtraction of the mean of samples from every point, should be omitted. In our method, since we have used mean subtraction *after* windowing in step two, the zero frequency has zero value but the effect of windowing to decrease the spectral leakage is low, therefore, the zero frequency magnitude is leaked across the whole spectrum. In Section IV, we introduce a novel general method for better discrimination using the zero frequency.

TABLE I
FOMS OF THE PULSES OBTAINED FROM VARIOUS DIGITIZERS, APPLYING FFT METHOD.

Digitizer	**8-bit, 1 GS**	**8-bit, 2 GS**	**12-bit, 250 MS**	**12-bit, 420 MS**
FoM	N/A	N/A	0.89	1.00

IV. DISCRIMINATION USING VARIABLE WINDOW

In this Section, we will use a known principle to implement a variable window for discrimination purposes. The principle used here is introduced in [4]. Let $n(i)$ and $g(i)$ be two discrete-time functions, both normalized to unity, i.e.

$$\sum_i n(i) = \sum_i g(i) = 1 \tag{2}$$

If we compute the time function of the relative difference between $n(i)$ and $g(i)$ (weights) as follows:

$$p(i) = \frac{g(i) - n(i)}{g(i) + n(i)} \tag{3}$$

then an unknown function $u(i)$, close to either $n(i)$ or $g(i)$, can be identified as one of them by the sign of S defined as:

$$S = \sum_i p(i)u(i) \tag{4}$$

In this article, we use this principle to design a window for discrimination of neutrons and gamma-rays. In Eqs. 2, 3, and 4, if we replace $n(i)$ and $g(i)$ with neutron and gamma-ray pulses, respectively, then if $S < 0$, the particle is identified as gamma-ray, and if $S > 0$, as neutron.

According to Eq. 3, those parts of the neutron and photon signals that differ most will have greater weights and the similar parts will have negligible weights. The similar segments could have weights with large absolute values when they are very close to zero; but according to Eq. 4, the final effect is minimal. Since the leading edges and the end-tail segments of neutrons and gamma-rays have almost the same shape, there will be insignificant weights or effects for corresponding points when these segments are included. However this minimal improvement of the discrimination caused by these segments will help us better identify the particles in low energy region. Inclusion of these parts is directly related to the capabilities of the hardware at hand. Omitting these segments will have the benefit of fewer number of multiplications (based

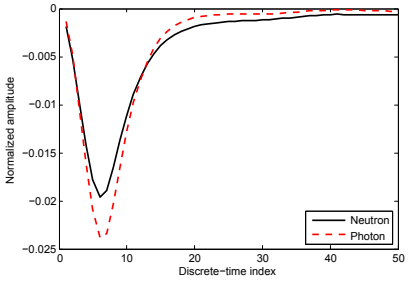

Fig. 7. Segments of neutron and gamma-ray pulses, obtained from DC440 digitizer (12-bit resolution, 420 MSamp/s), when normalized to unity (using Eq. 2).

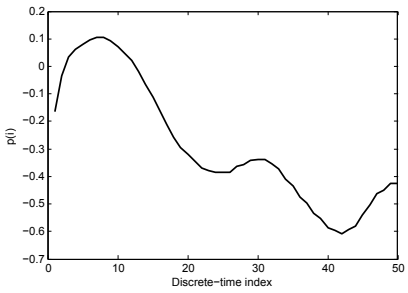

Fig. 8. Weight function $p(i)$, obtained from Eq. 3 using the two signal segments shown in Fig. 7.

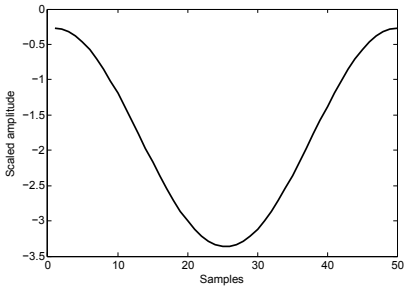

Fig. 9. Hamming window with its amplitude scaled according to Eq. 6 for a specific pulse under process.

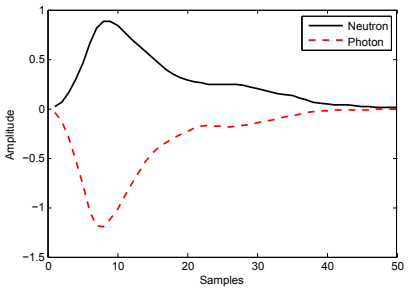

Fig. 10. Segments of neutron and photon pulses after application of their corresponding scaled Hamming windows.

on Eq. 4), but a slight decrease in the quality of the results. For this work, the area of interest starts from the point where the rising edge hits the 1% threshold level and the end point is a constant number of samples after this starting point for all signals, such that this interval covers a signal as much as possible.

In Eq. 3, a sample gamma-ray $g(i)$ and a sample neutron $n(i)$ are picked and used to build the weights. These samples need to be patterns representing the types of pulses contained in the whole data set. Therefore, more than one sample should be used for each pulse type to obtain better results. If we use k number of pulses ($k > 1$) from each radiation type to build the sample pulses required, then

$$\begin{aligned} g(i) &= \frac{\sum_{j=1}^{k} g_j(i)}{k} \\ n(i) &= \frac{\sum_{j=1}^{k} n_j(i)}{k} \end{aligned} \tag{5}$$

Once every point of the two sample pulses are built using the Eqs. 5, they are normalized to unity using the Eq. 2 (as Fig. 7 illustrates), and then applied to the Eq. 3 to build the weight sequence (as shown in Fig. 8).

We use the constant weight sequence $p(i)$, in conjunction with every arriving pulse, to scale a varying Hamming window. If $u(i)$ is the unknown pulse to be processed, it is passed along with $p(i)$ to Eq. 4 to compute S. As mentioned before, S serves as the identifier for the pulse and hence can itself be used as counting/discriminating factor. However, S could also be used to scale a window which is in turn used to count/discriminate. In order to preserve the scaling factor S after applying window to the pulse, S should be divided by $u(m)$, the median of the unknown sequence $u(i)$, where the peak of the window lies:

$$\text{Scale} = \frac{S}{u(m)} \tag{6}$$

However, Eq. 6 only scales the magnitude, not the sign, hence could be ignored. A sample Hamming window scaled in this manner for a specific neutron pulse is shown in Fig. 9.

A pulse is easily identified when its correspondingly-built window is applied to it. The direction of the pulse amplitude reveals its identity; Using Eq. 3, neutrons will have positive amplitudes while photons will have negative ones. This can be used to count the number of neutrons and photons in an experiment. Fig. 10 shows two sample windowed neutron and photon pulses. Since the zero base-line is the separator between these signals, to find the efficiency of discrimination, an ideal factor to use would be the sum of a pulse sequence points. This sum is the DC value or the zero frequency of the windowed pulse. The choice of Hamming window for this application is clear now: pedestal raised property of this window pushes the two signal types far from each other on the two sides of zero baseline. However, the other window types like Hanning would perform well too.

The double-sided amplitude spectra of neutron and gamma-ray signals in Fig. 10 are shown in Fig. 11; zero frequency can easily discriminate the two signal types. Fig. 12 illustrates the experimental distribution plot of neutrons and photons for the data obtained from DC440 digitizer with 12-bit resolution and set at 420 MSamp/s frequency rate. As seen, the zero discrimination value is the separator here; neutrons have positive and gamma-rays have negative discrimination values. Tab. II shows the FoM (computed using Eq. 1) and neutron and photon counts for this data set. The discrimination quality is improved in this method compared to the application of FFT

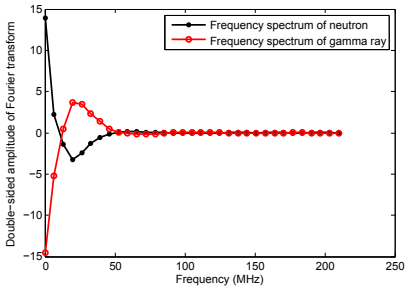

Fig. 11. The double-sided amplitude spectra of the γ-ray and neutron events shown in Fig. 10, applying a 64-point FFT. The pulses are obtained using DC440 digitizer (12-bit resolution, 420 MSamp/s).

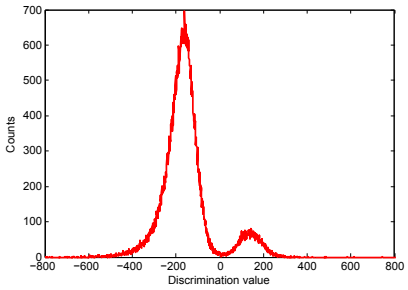

Fig. 12. Discrimination of photon and neutron signals using variable window. The pulses were obtained using DC440 digitizer (12-bit resolution, 420 MSamp/s).

TABLE II
FOM AND COUNTS OF THE PULSES OBTAINED FROM DC440 DIGITIZER.

Data format	FoM	Neutron counts	Photon counts
12-bit, 420 MSamp/s	1.20	9149	90851

TABLE III
FOMS AND COUNTS OF THE PULSES OBTAINED FROM DC440 AND DP210 DIGITIZERS UNDER DIFFERENT SAMPLING RATES.

Data format	FoM	Neutron counts	Photon counts
12-bit, 250 MSamp/s	1.13	8807	91193
8-bit, 1 GSamp/s	1.12	9725	90275
8-bit, 2 GSamp/s	1.04	9204	90796

method, explained in Section III. FoMs and pulse counts for the other data sets with different resolutions and frequency rates are shown in Tab. III. While FFT method, explained previously, failed to discriminate low-resolution data, this method discriminates these pulses very efficiently.

V. DISCUSSION

Two important factors affecting the FoM of a discrimination method are resolution and sampling rate of the digitizer. According to Nyquist criterion, the sampling rate must be greater than twice the bandwidth of continuous digitizer input signal. The FFT of the recorded neutron and photon signals indicates frequency components up to 100 MHz [5]. Therefore, the minimum necessary sampling frequency for neutron and photon signals is about 200 MS/s. The exact impact of the sampling rate on the separation quality of a specific method depends on how the method functions, and estimation of this effect can be involved. For the approaches introduced in this article, while increasing the low sampling rate of 250 MHz (which is close to the minimum 200 MHz required) to 420 MHz increases FoM, as Tabs. I, II and III show, increasing from the high sampling rate of 1 GHz to 2 GHz does not improve the FoM.

The factor with a greater impact on discrimination quality is digitizer resolution. The process of converting a discrete-time continuous-amplitude signal into a digital signal by expressing each sample value as a finite number of digits is called quantization. The resolution (or quantization step size) is the distance between two successive quantization levels. The error introduced in representing the continuous-valued signal by a finite set of discrete value levels is called quantization error or quantization noise. The quality of the digitizer output could be measured by signal-to-quantization noise ratio (SQNR). Since quantization errors of neutron and photon signals are almost uniformly distributed over the quantization interval, the following well-known equation [6] reliably estimates the quality of a b-bit digitizer output:

$$SQNR(dB) = 1.76 + 6.02b \tag{7}$$

Eq. 7 implies that SQNR increases approximately 6 dB for every bit added to the digitizer word length. This relationship gives the number of bits required by an application to assure a given signal-to-noise ratio.

In order to verify the performances of the novel methods introduced in this article, we apply PGA method to the same pulses datasets as used for the methods in this paper. PGA method, introduced in [3], is recognized as an efficient n/γ discrimination method with a high FoM. The slower decay of the light function of a scintillator for a neutron interaction than that for a γ-ray interaction is exploited in this method. The gradient between the peak amplitude and the amplitude a specified time after the peak amplitude (called the discrimination amplitude) on the trailing edge of the pulses are compared and used as the discrimination factor. Fig. 13 illustrates the peak and discrimination amplitudes on neutron and photon signals. The gradient is calculated using

$$m = \frac{\Delta y}{\Delta t} = \frac{(y_p - y_d)}{(t_p - t_d)} \tag{8}$$

where m, y_p, y_d, t_p, and t_d are the gradient, the peak amplitude (which is a constant for normalized pulses), the discrimination amplitude, the time of peak amplitude occurrence, and the time of discrimination amplitude occurrence, respectively. For this work, we used some training pulses to locate the best discrimination amplitude, which occurred about 36 ns after the peak of the pulse. In general, the optimal timing for the discrimination amplitude which makes the highest difference between the two radiation types is dependent on the scintillator properties and also on the PMT. The FoMs obtained are listed in Tab. IV. A comparison shows that the novel methods introduced here are either better or have almost the same discrimination quality as the PGA method does. Fig. 14 shows the best discrimination plot obtained by PGA method.

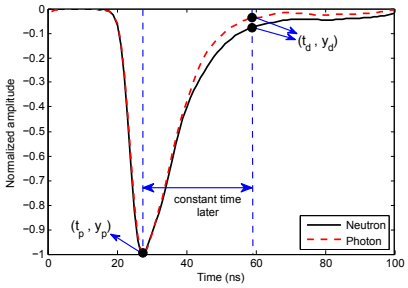

Fig. 13. The points on smoothed neutron and photon signals used in PGA discrimination method.

TABLE IV
FOMS OF PGA METHOD FOR THE PULSES OBTAINED FROM VARIOUS DIGITIZERS.

Digitizer	8-bit, 1 GS	8-bit, 2 GS	12-bit, 250 MS	12-bit, 420 MS
FoM	0.88	0.91	0.94	1.00

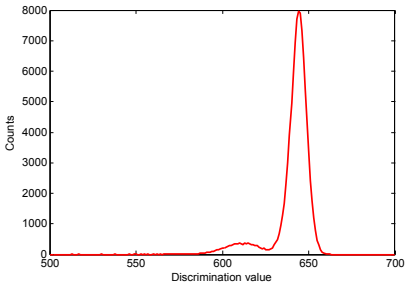

Fig. 14. Discrimination of photon and neutron signals, applying PGA method. The pulses are obtained using DC440 digitizer (12-bit resolution, 420 MSamp/s).

VI. CONCLUSION

In this article, we introduced two novel algorithms to discriminate the neutron and photon pulses captured in a mixed environment. Two digitizers, each featuring a different resolution and each set at two different sampling rates, were used to observe the reaction of each method to the data sampling conditions. While the application of FFT method is promising only for the data recorded with high resolution, the counting/discriminating using variable window is robust.

Since both discrimination approaches presented in this article are computationally simple, typical embedded system technologies could be easily used for realization. Moreover, in many industrial applications, neutron/gamma discrimination is required to be done in real-time fashion. Discrimination of the pulses through a simple method brings about quickness needed for real-time operations.

REFERENCES

[1] S. Budakovsky, N. Galunov, B. Grinyov, N. Karavaeva, J. K. Kim, Y.-K. Kim, N. Pogorelova, and O. Tarasenko, "Stilbene crystalline powder in polymer base as a new fast neutron detector," *Radiation Measurements*, vol. 42, no. 4-5, pp. 565 – 568, 2007, proceedings of the 6th European Conference on Luminescent Detectors and Transformers of Ionizing Radiation (LUMDETR 2006). [Online]. Available: http://www.sciencedirect.com/science/article/pii/S1350448707001564

[2] G. Ranucci, "An analytical approach to the evaluation of the pulse shape discrimination properties of scintillators," *Nuclear Instruments and Methods in Physics Research Section A: Accelerators, Spectrometers, Detectors and Associated Equipment*, vol. 354, no. 2-3, pp. 389 – 399, 1995. [Online]. Available: http://www.sciencedirect.com/science/article/pii/0168900294008868

[3] B. Mellow, M. Aspinall, R. Mackin, M. Joyce, and A. Peyton, "Digital discrimination of neutrons and g-rays in liquid scintillators using pulse gradient analysis," *Nuclear Instruments and Methods in Physics Research Section A*, vol. 578, no. 1, pp. 191–197, 2007.

[4] E. Gatti and F. de Martini, "A new linear method of discriminating between elementary particles in scintillation counters," in *Int. Symp. Nuclear Electronics*, vol. 2, Belgrade, 1961, pp. 265 – 276.

[5] F. Belli, B. Esposito, D. Marocco, and M. Riva, "A study on the pulse height resolution of organic scintillator digitized pulses," *Fusion Engineering and Design*, vol. 88, no. 68, pp. 1271 – 1275, 2013, proceedings of the 27th Symposium On Fusion Technology (SOFT-27); Liége, Belgium, September 24-28, 2012. [Online]. Available: http://www.sciencedirect.com/science/article/pii/S092037961200587X

[6] J. G. Proakis and D. G. Manolakis, *Digital Signal Processing, Fourth Edition*. Upper Saddle River, New Jersey 07458: Prentice Hall, 2006.